RESEARCH ARTICLE

ADVANCED OPTICAL MATERIALS
www.advopticalmat.de

A Versatile Method for Nano-Fabrication on Diamond Film: Flexible Diamond Metasurfaces as a Demonstration

Yicheng Wang, Jixiang Jing, Yumeng Luo, Linjie Ma, Xiaomin Wang, Yuhao Zhang, Dong-Keun Ki, Zhongqiang Wang, Qi Wang, Kwai Hei Li,* and Zhiqin Chu**

Diamond exhibits unique performance across a wide range of applications due to its enormous presentable properties in electronic, photonic, and quantum fields. Yet heterogeneous integration of diamonds for on-chip functionalities, like 2D materials, remains challenging due to the hard acquisition of scalable, transferable, and ultrathin diamond samples. Recently, edge-exposed exfoliation is demonstrated as an effective way to produce wafer-scale, freestanding, and ultrathin diamond films. However, the incompatibility of the newly developed diamond film with conventional nano-fabrication methods makes it difficult to fabricate diamond film into practical devices. Herein, the mask-transferring by sugar is demonstrated as a versatile method for pattern-definition on diamond films, which shows satisfying geometrical resolution and accuracy comparing to conventional approaches. Additionally, based on this method, the flexible all-diamond metasurfaces functioning as structural colors are achieved, which indicates its wide potential for fabricating more diamond-related devices.

1. Introduction

Diamond is widely proposed for future electronic and photonic technologies due to its superlative material properties including large bandgap, high carrier mobility, thermal conductivity,[1,2] and ultrawide optically-transparent window from infrared to ultraviolet. However, heteroepitaxial growth of diamond on arbitrary substrates remains difficult, hindering the integration and evolution of diamond-based technologies. To build diamond heterogeneous platforms for expanding on-chip functionalities, including electronics (e.g., transistors,[3–6] P-N junctions[7,8]), photonics (e.g., waveguides,[9–11] resonators,[12–14] metasurfaces,[15–18] metalens[19–21]), and quantum sensors (e.g., thermometers,[22–25] magnetometers,[26–28]), the integrable and ultrathin diamond is urgently needed. Despite extensive efforts that have been made over the past decades, producing large quantities of desired ultrathin and transferable diamond film for widespread use still remains challenging.

Currently, edge-exposed exfoliation using sticky tape has been demonstrated as a simple, scalable, and reliable method for massively producing ultrathin and transferable diamond films.[29] However, as a newly developed 3D film, it is still difficult for the post-manipulation of ultrathin diamond (e.g., on-surface nanofabrication) referring the way of 2D materials and bulk materials via conventional methods (e.g., lithography and etching). The incompatibility of the diamond film with conventional nanofabrication process mainly attributed to its special properties, including i) low surface electrical conductivity, which suffers from proximity effect and charge accumulation, easily inducing the aggregation of electrons when conducting electron-beam-lithography (EBL), diminishing the accuracy of defined pattern, ii) fragility that leaves shattering and cracking due to the stress during directly spin-coating on diamond film, especially for films with a thickness thinner than one micron, undermining its integrity, and iii) surface geometric fluctuation when attached to curved and flexible surfaces, which could easily lead to uneven distributions of spin-coated resists and simultaneously bring difficulties in sample focusing when implementing photo-/e-beam lithography. Despite those strategies have been proposed to replace conventional wafer-fabrication processes including transfer printing,[30–32] metal or conductive polymer coating[33,34] for anti-charge accumulation,

Y. Wang, J. Jing, L. Ma, Y. Zhang, Z. Chu
Department of Electrical and Electronic Engineering
The University of Hong Kong
Pokfulam, Hong Kong, China
E-mail: zqchu@eee.hku.hk

The ORCID identification number(s) for the author(s) of this article can be found under https://doi.org/10.1002/adom.202403429

DOI: 10.1002/adom.202403429

Y. Luo, K. H. Li
School of Microelectronics
Southern University of Science and Technology
Shenzhen 518055, China
E-mail: khli@sustech.edu.cn

X. Wang, D.-K. Ki
Department of Physics
The University of Hong Kong
Pokfulam, Hong Kong, China

Z. Wang, Q. Wang
Dongguan Institute of Opto-Electronics
Peking University
Dongguan 523808, China
E-mail: wangq@pku-ioe.cn

self-assembly nanospheres,[35,36] nano-imprint lithography.[37–39] However, those methods still encounter limitations such as uneven distribution of conductive polymer, chemical contaminations to diamond and substrate, and challenges in the removal of deposited metals without damaging the diamond sample and substrate.

In this study, we demonstrate mask-transferring by sugar as a versatile method to help conduct high-precision, large-scale, repeatable nano-fabrication on our developed diamond films. Particularly, utilizing sugar as the transfer medium, we can successfully transfer the pre-defined patterns to diamond films as masks, and conduct diamond etching subsequently. This approach is straightforward, non-polluting, and highly accurate, unlocking the vast possibility of diamond film applications. As a-proof-of photonic application, the structural color based on all-diamond metasurfaces on flexible polyethyleneglycol-terephthalate (PET) substrate is showcased. Related characterizations indicate the diamond-based structural colors exhibit higher reflectance, better color saturation, and wider color gamut than previous works,[16,40–43] which is also stable and robust under different extents of flexible deformations, making it possible for high-quality[44] and stable display[45,46] applications. This developed sugar-transfer method opens a new way of high-precision nanofabrication on transferable diamond films, and will undoubtedly boost the development of diamonds in diverse fields.

2. Results and Discussion

2.1. A Versatile Method for Nano-Fabrication on Diamond Film

The diamond film with ≈600 nm thickness was first grown by microwave plasma chemical vapor deposition (MPCVD) method on the silicon substrate (see Experimental Section). When attaching the sticky tape on the surface of the diamond and stretching it at a moderate speed, the diamond film could be gradually peeled off from the silicon substrate,[29] as shown in **Figures** 1a and S1 (Supporting Information). Photographs of diamond-on-silicon assembly and exfoliated diamond film are shown in Figure 1b,c, respectively, where a 2-inch size was achieved. High-magnification scanning electron microscope (SEM) images (Figure 1d,e) and atomic force microscope (AFM) images (Figure 1f,g) present the surface morphology of two sides of exfoliated diamond films, and corresponding surface amplitude along the white dashed lines in Figure 1f,g are presented in Figure 1h,i. Compared with the rough as-grown (top) surface (Ra = 44.58 nm), the buried (bottom) surface exhibits extremely lower roughness (Ra: ≈1 nm) that is seldomly mentioned by others. This discovered ultra-flat surface without experiencing any post-flattening process (e.g., mechanical or chemical polishing) makes it accessible to high-precision nanofabrication, overcoming the bottleneck of the rough as-grown surface for widespread use in the long term (Figure S2, Supporting Information).

After acquiring the scalable, ultra-flat diamond film, it still remains difficult to conduct high-precision nanofabrication on its surface when following conventional fabrication methods including photolithography and E-beam lithography (Details see Section S3, Supporting Information). To unleash the limitation of the conventional wafer-fabrication process, we herein introduce a versatile method to conduct nanofabrication on diamond film by sugar transferring, which can achieve large-area, high-precision, and good repeatability. The schematic illustration of our proposed method is shown in **Figure** 2, which can be generally classified into three steps: i): Mask preparation: Utilizing E-beam lithography to acquire a designed mask on indium-tin-oxide (ITO) film substrate (see Experimental Section), ii) Sugar transfer: to effectively transfer the fabricated pattern to the diamond surface, a mixture of corn syrup, cane sugar and deionized water was prepared.[30] By dropping sufficient sugar solution (5–10 µL) on top of the fabricated template pattern on ITO film, and then putting them inside of a heating oven at 70 °C for several hours, the sugar solution would be solidified. Notably, excessively low and high temperatures could induce overlong solidifying time and residual bubbles, respectively, damaging the template pattern. Next, by slightly bending the PET film, the solid sugar would be easily detached from the film where the residual stress on dried sugar may assist the separation[30] without needing any sacrificial layer, iii) Diamond etching: By placing the dried sugar on diamond film and gently pressing it with tweezer, the diamond film would be conformed to the flat surface of sugar. The sugar was subsequently dissolved away with deionized water, leaving designed masks on diamond film. Inductive coupled plasma (ICP) was employed for diamond etching where the flow rate of oxygen gas, RF voltage, bias voltage, and cavity pressure was set to 80 sccm, 200 W, 60 W, and 10 mTorr, respectively. Finally, the fabricated diamond pattern would be obtained after removing the masks by a KOH solution. Utilizing a predefined mask on conductive ITO film, difficulties of direct exposure on diamond film (e.g., diamond film's fragility, uneven distribution of resist, and problems with focusing) can be avoided, and the entire transfer procedure is chemicals-free to diamond film and the substrate, which avoids contaminations from damaging the device and substrate.

2.2. Comparison Between our Proposed Method and Conventional Method

Figure 3a shows the schematic illustration comparing the mask preparation procedure using our proposed method and conventional method, where our proposed method utilized the aforementioned sugar-transfer technique, and the conventional method involved spin-coating of resist and E-beam lithography directly on diamond film. Figure 3b–g presents the SEM images of fabricated masks on the buried surface of diamond film utilizing our method (b–d) and conventional lithography method (e–f), respectively. Particularly, the circular pillar arrays by sugar-transferring (Figure 3b) possess more regular morphology than that obtained by direct lithography (Figure 3e). In addition, the fabricated nano-gratings also demonstrate the superiority of our proposed sugar-transferring method. Different magnification SEM images (Figure 3c,d) indicate the well-defined morphology (e.g., accurate parameter as designed, and clear boundaries) of nano-gratings by sugar transferring. In contrast, nano-gratings obtained by conventional direct lithography (Figure 3f,g) exhibit geometrical distortion that deteriorates from the edge of the pattern toward the center. The unsatisfying outcomes from

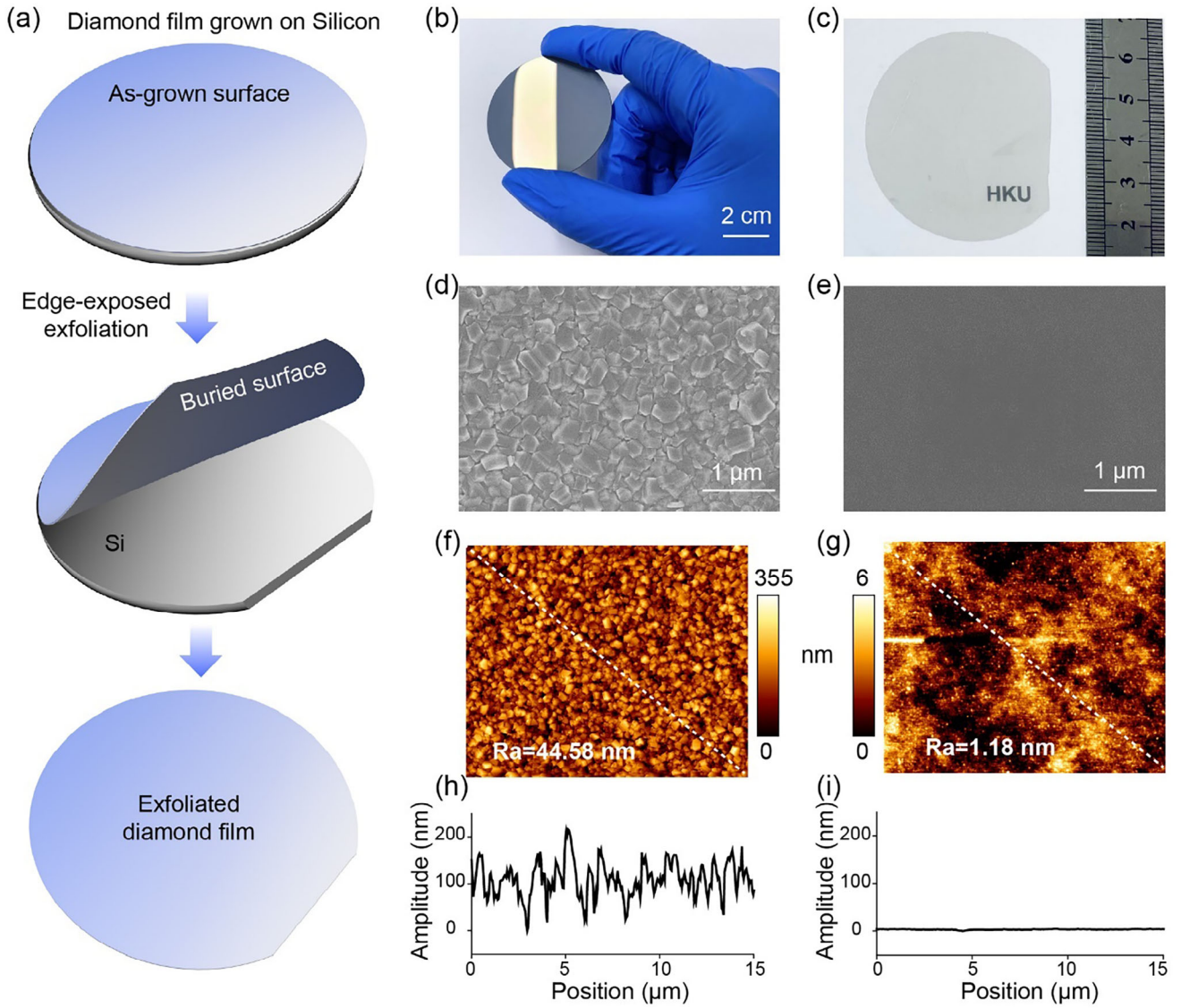

Figure 1. a) Schematic diagram of exfoliating diamond film from the silicon wafer. b,c) Photograph of the 2-inch diamond-on-silicon wafer (b) and exfoliated diamond film (c), respectively. d,e) SEM images of as-grown surface (d) and buried surface (e) of diamond film. f,g) AFM images of as-grown surface (f) and buried surface (g) of diamond film. h,i) Corresponding surface amplitude along the white dashed lines in (f) and (g), respectively.

direct exposure mainly attributed to charge accumulation and proximity effect during EBL exposure, as well as surface geometric fluctuation of the diamond-tape platform, which would affect the uniformity of spin-coated photo/e-beam resist and bring difficulties in focusing E-beam in a macro scale during exposure (Section S3, Supporting Information).

3. Flexible Structural Colors Based on All-Diamond Metasurfaces

After demonstrating the feasibility of our sugar-transferring method, the performance of the fabricated diamond-based device should be further demonstrated. Despite the superior characteristics of diamonds in the field of photonics and optics, to the best of our knowledge, diamond-based metasurfaces have been seldomly reported up to now. Therefore, the structural colors based on Mie's resonance effect is showcased for all-diamond flexible metasurfaces. Compared with traditional metallic structural colors who suffer from high absorption at the blue region, and dielectric (e.g., Si, TiO_2) structural colors that are prone to corrosion, diamond material emerges as a promising candidate of photonic devices due to its high refractive index, negligible extinction coefficient,[29,43] and exceptional chemical and mechanical durability.

Figure 4a shows the schematic unit cells of diamond metasurfaces, which are composed of diamond pillars and PET tape substrate, where *p* and *g* denote the period of the diamond pillar array and the gap between adjacent diamond pillars, respectively. Figure 4b exhibits a top-view SEM image of fabricated diamond

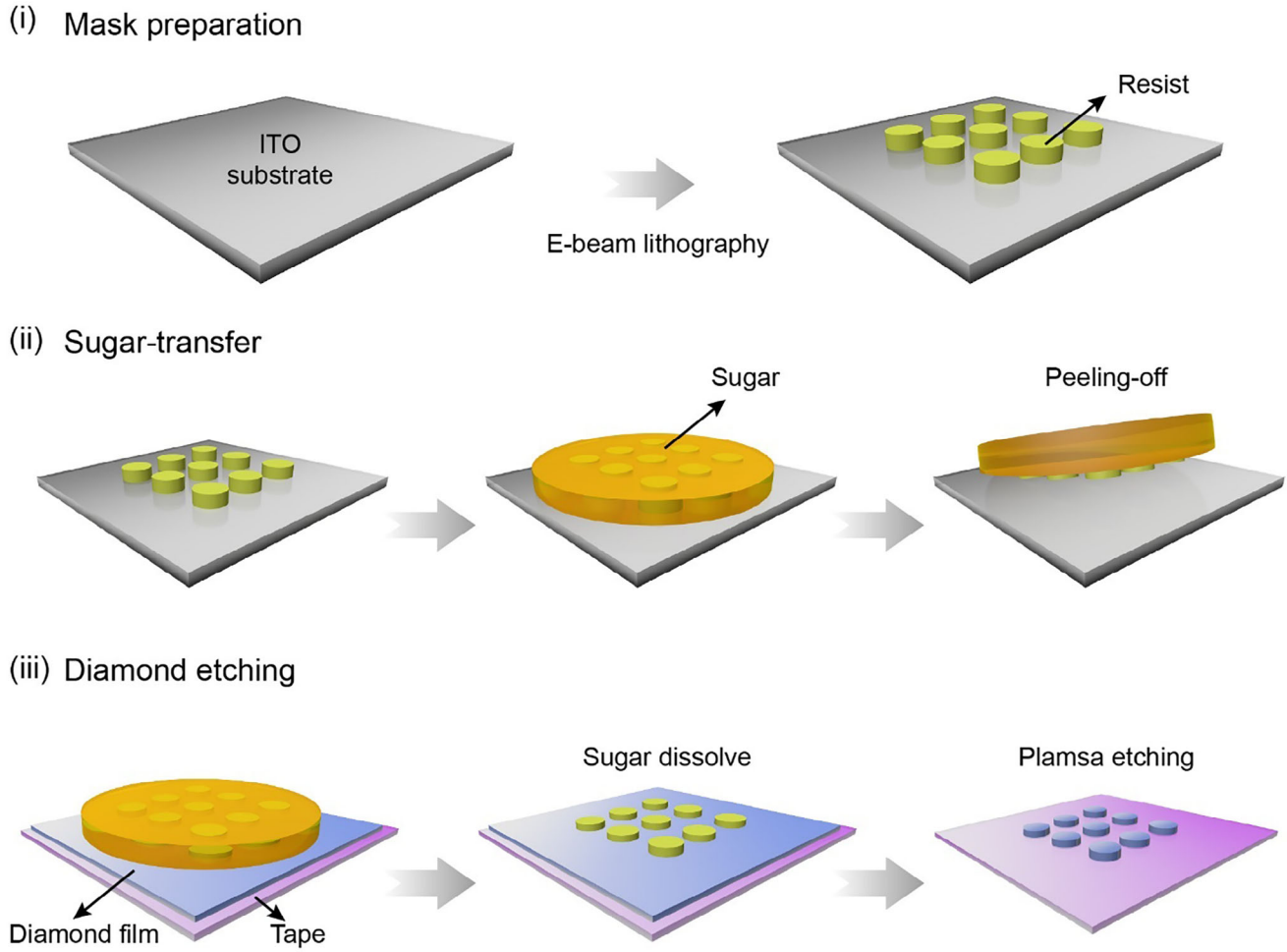

Figure 2. Schematic illustration of nano-fabrication on diamond film using our proposed sugar-transfer method.

pillar arrays with the period $p = 400$ nm and gap $g = 100$ nm. The measured refractive index and extinction coefficient of the diamond film are shown in Figure 4c. Figure 4d presents the color palette of fabricated diamond structural colors by adjusting the period p and gap g from 280 to 400 nm and 90 to 140 nm, respectively. In particular, the color would change from blue to red as g decreases and p increases, covering the entire visible range. Derived from one row of the color palette (marked in red box), the measured reflectance spectra also behaved the obvious redshift, as shown in Figure 4e. Specifically, the reflectance intensity was up to 88.78% when setting g and p as 100 and 370 nm. Figure 4f exhibits the positions of fabricated diamond structural colors in the standard CIE 1931 color map, which indicates their satisfactory color saturation and wide gamut. Due to the flexible PET substrate, the proposed structural color can be bended and conformed to curved surfaces. Figure 4g,h present photograph and zoomed-in microscope images of diamond structural color under relaxed status and bended status, respectively. Where the diamond structural color is attached onto a piece of black fiber to avoid background light. The subtle difference of reflectance spectra between relaxed and different bending status (Section S4, Supporting Information) indicates the proposed diamond structural color possesses solid stability under deformation. The satisfying saturation and ultra-high reflectance intensity compared with previews works,[16,40–42,47] as well as the stable display characteristics further underscore the decent performance of diamond film and the adequate compatibility of our proposed method for high-precision nano-fabrication, which shows promising potential toward applications including high-performance displays,[47] encryptions,[16,46] flexible and wearable display,[48] durable display devices for harsh environments,[49] etc.

4. Conclusion

In this study, we proposed a versatile method for nano-fabrication on our newly developed ultrathin and flexible diamond film, which overcomes the challenges and limitations of conventional nano-fabrication method for 2D materials and bulk materials. Our proposed method involves the straightforward transfer of masks from ITO film to diamond film without the need of extra chemicals, thereby preventing diamond film and substrate from being damaged or contaminated. Compared with masks fabricated by conventional method, our results exhibit higher geometrical resolution and better repeatability, as well as the capability of fabricating large-scale structures. As a demonstration, a

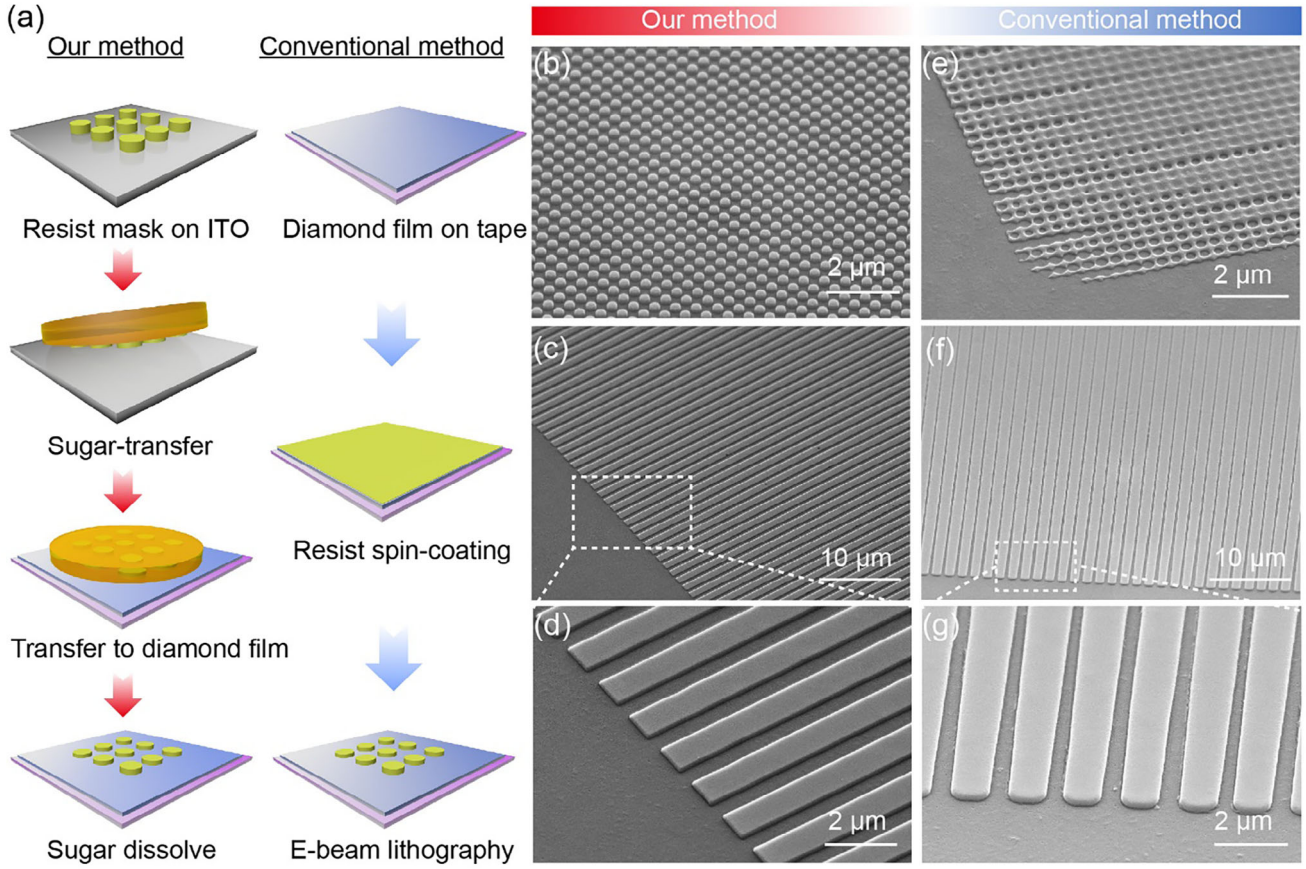

Figure 3. a) Schematic illustration of our sugar-transferring method and conventional method for fabricating mask pattern on diamond film. b,e) SEM images of circular array masks with a period of 400 nm made on diamond film's buried surface using our method (b) and conventional method (e), respectively. c,f) SEM images of grating masks made on diamond film's buried surface using our method (c) and conventional method (f), respectively. d,g) Zoomed in images of (c) and (f).

flexible all-diamond metasurface functioning as structural colors is carried out, which is the first flexible device made with diamond film, the structural colors exhibit decent properties including ultra-high reflectance intensity up to 88.87%, a wide gamut spanning the entire visible spectrum, satisfying saturation, and stable display under bending. It is believed to hold great promise for stable and high-quality structural colors, wearable displays, and information encryptions. The good performance of the fabricated diamond structural color further substantiates the superiority of the proposed method, unlocking the vast potential applications of diamond films in areas such as diamond photonics, next-generation electronics devices, quantum sensing, heat spreaders, etc.

5. Experimental Section

CVD Growth of Diamond Film: The heteroepitaxial growth of diamond on a silicon (Si) substrate encompasses three essential steps: substrate pretreatment, diamond seed deposition, and chemical vapor deposition (CVD) of diamond membranes. Initially, the Si surface underwent hydrogen plasma treatment. A 2-inch silicon wafer was then introduced into a microwave plasma-assisted chemical vapor deposition (MPCVD) device for 10 min with settings of 1300-W power, 35-Torr cavity pressure, and a 300-sccm hydrogen (H_2) gas flow. Preparing the diamond seeds required a series of mixing, dispersing, and centrifuging steps. Diamond seeds (sourced from Tokyo Chemical Industry Company Limited) smaller than 10 nm were mixed with dimethyl sulfoxide (DMSO), anhydrous ethanol, and acetone at a mass ratio of 1:5000:250:250. This mixture was sonicated for 12 h to ensure proper dispersion, followed by centrifugation at 1000 rpm for 20 min to eliminate impurities. The suspension was then spin-coated onto the Si wafer under the following conditions: an initial spin at 500 rpm with three drops added within 15 s, followed by an increase to 4500 rpm for 110 s. This spin-coating process was repeated three times. Finally, the wafer with the deposited diamond seeds was placed into the MPCVD setup (Seki 6350) for diamond membrane growth. The primary parameters for growing a 1-μm-thick diamond membrane included 3400-W microwave power, a temperature of 900 °C, a 15-sccm methane flow rate, and a 40-min growth period.

Mask Preparation: A PET film (1.25-mm thick) with 200 nm-surface deposition of electrically conductive ITO was firstly cut into small pieces of 1 cm × 1 cm size by scissors. The hydrogen silsesquioxane (HSQ) was then spin-coated on the surface of PET film at a spinning rate of 4500 r min^{-1} for 60 s, followed by 80 °C heating for 180 s. After spin-coating of E-beam resist, EBL was carried out for pattern definition at a dose of 750 μJ cm^{-2}, followed by development in 25% Tetramethylammonium hydroxide (TMAH) for 60 s.

Simulation of Diamond Metasurfaces: Software Lumerical FDTD solutions were used to calculate the theoretical reflectance of diamond

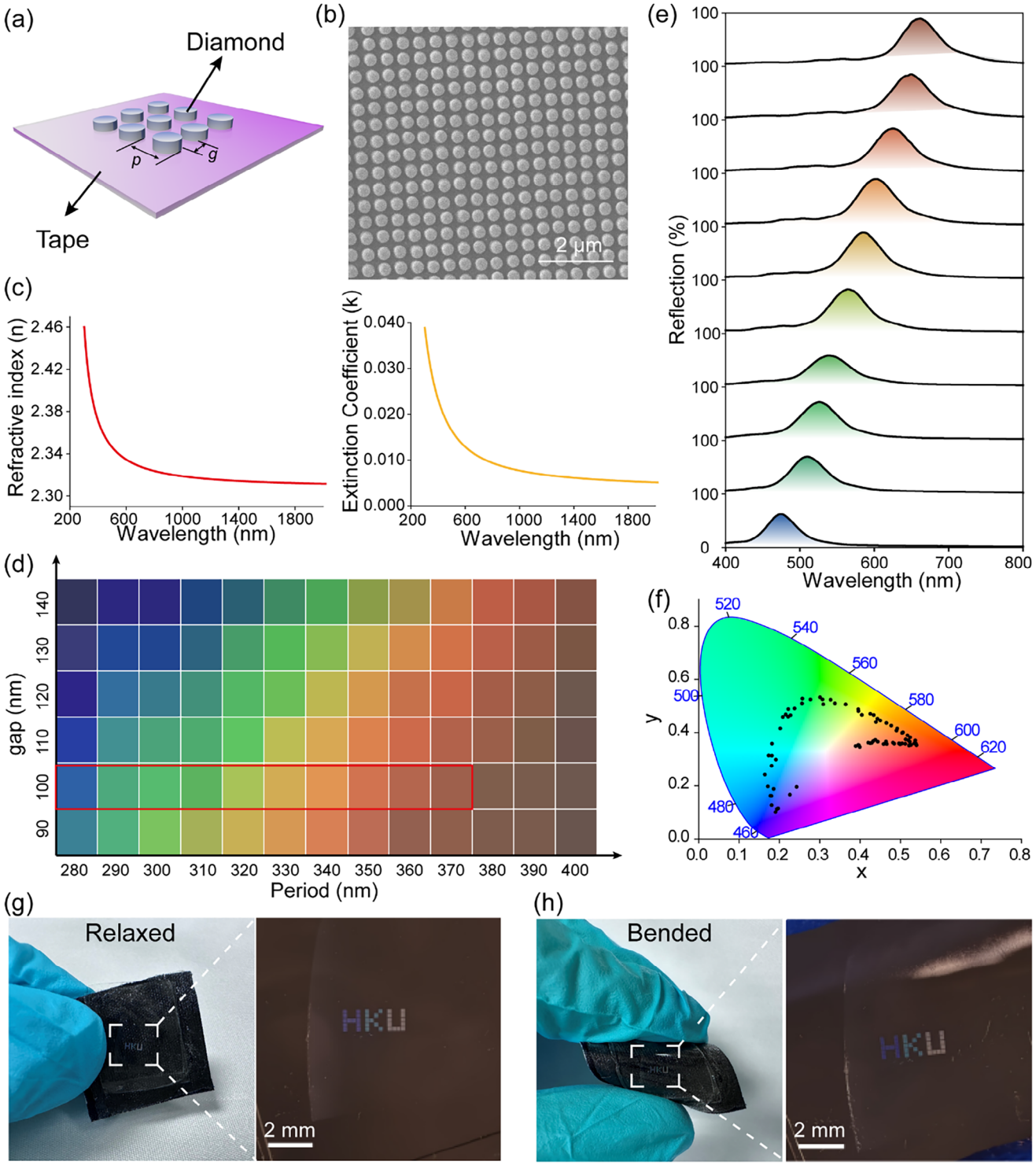

Figure 4. a) Schematic unit cells of diamond metasurfaces on tape substrate. b) Top-view SEM image of diamond metasurfaces. c) Measured refractive index and extinction coefficient of the diamond film. d) The color palette of fabricated diamond structural colors. e) Corresponding experimental reflectance spectra of diamond structural colors (red mark in (d)), where the period *p* varies from 280 to 370 nm at a fixed *g* of 100 nm. f) CIE 1931 color map of fabricated structural colors. g,h) Photograph and zoomed-in microscope images of diamond structural colors under relaxed and bended status, respectively.

structural color based on the finite-difference time-domain (FDTD) method, periodic boundary condition was adopted at the *x*- and *y*- direction from the top view of diamond structural color to simulate the periodic distribution of diamond unit cells, perfectly matched layer (PML) boundary condition was adopted at the *z*-axis to serve as absorber to block outgoing electromagnetic wave.

Supporting Information

Supporting Information is available from the Wiley Online Library or from the author.

Acknowledgements

Y.W. and J.J. contributed equally to this work. K.H.L. acknowledges the Shenzhen Fundamental Research Program (JCYJ20220530113201003). Z.C. acknowledges the financial support from the National Natural Science Foundation of China (NSFC) and the Research Grants Council (RGC) of the Hong Kong Joint Research Scheme (Project No. N_HKU750/23), HKU seed fund, and the Health@InnoHK program of the Innovation and Technology Commission of the Hong Kong SAR Government. Q. W. acknowledges the Guangdong Major Project of Basic and Applied Basic Research (2023B0303000012), Natural Science Foundation of China (62471011).

Conflict of Interest

The authors declare no conflict of interest.

Data Availability Statement

The data that support the findings of this study are available from the corresponding author upon reasonable request.

Keywords

diamond film, diamond metasurface, flexible display, nano-fabrication, structural color

Received: December 13, 2024
Revised: March 8, 2025
Published online: April 19, 2025

[1] A. Broda, A. Kuzmicz, G. Rychlik, K. Chmielewski, A. Jedlinska, I. Sankowska, K. Malec, K. Michalak, J. Muszalski, *Opt. Quant. Electron.* **2017**, *49*, 287.
[2] H. Ichikawa, K. Yamaguchi, T. Katsumata, I. Shoji, *Opt. Express.* **2017**, *25*, 22797.
[3] N. Suntornwipat, S. Majdi, M. Gabrysch, K. Kovi, V. Djurberg, I. Friel, D. Twitchen, J. Isberg, *Nano Lett.* **2021**, *21*, 868.
[4] T. Iwasaki, Y. Hoshino, K. Tsuzuki, H. Kato, T. Makino, M. Ogura, D. Takeuchi, T. Matsumoto, H. Okushi, S. Yamasaki, M. Hatano, *Appl. Phys. Express* **2012**, *5*, 091301.
[5] H. Kawarada, H. Tsuboi, T. Naruo, T. Yamada, D. Xu, A. Daicho, T. Saito, A. Hiraiwa, *Appl. Phys. Lett.* **2014**, *105*, 013510.
[6] M. Syamsul, Y. kitabayashi, D. Matsumura, T. Saito, Y. Shintani, H. Kawarada, *Appl. Phys. Lett.* **2016**, *109*, 203504.
[7] C. Masante, M. Kah, C. Hebert, N. Rouger, J. Pernot, *Adv. Electron. Mater.* **2022**, *10*, 1002.
[8] A. Tajani, C. Tavares, M. Wade, C. Baron, E. Gheeraert, E. Bustarret, S. Koizumi, D. Araujo, *Phys. Stat. Sol.* **2004**, *201*, 2462.
[9] N. Yavuz, M. Bayer, H. Cirkinoglu, A. Serpenguzel, T. Phu, A. Giakoumaki, V. Bharadwaj, R. Ramponi, S. Eaton, *Molecules* **2020**, *25*, 2698.
[10] A. Lopez-Lorente, P. Wang, M. Sieger, E. Catalen, M. Karlsson, F. Nikolajeff, L. Osterlund, B. Mizaikoff, *Phys. Status Solidi* **2016**, *213*, 2117.
[11] M. Bhaskar, D. Sukachev, A. Sipahigil, R. Evans, M. Burek, C. Nguyen, L. Rogers, P. Siyushev, M. Metsch, H. Park, F. Jelezko, M. Loncar, M. Lukin, *Phys. Rev. Lett.* **2017**, *118*, 223603.
[12] A. Sartori, P. Belardinellli, R. Dolleman, P. Steeneken, M. Ghatkesar, J. Buijnsters, *Small* **2019**, *15*, 1803774.
[13] B. Regan, A. Trycz, J. Froch, O. Schaeper, S. Kim, I. Aharonovich, *Nanoscale* **2021**, *13*, 8848.
[14] G. Joe, C. Chia, B. Pingault, M. Haas, M. Chalupnik, E. Cornell, K. Kuruma, B. Machielse, N. Sinclair, S. Meesala, M. Loncar, *Nano Lett.* **2024**, *24*, 6831.
[15] J. Jing, Y. C. Yiu, C. Chen, D. Lei, L. Shao, Q. Wang, K. H. Li, N. Wong, Z. Chu, *Adv. Photonics Res.* **2022**, *3*, 2100292.
[16] J. Gu, Y. Liu, N. Meng, V. Sahmuganathan, S. Tan, J. Sudijono, J. Tang, E. Venkatasubramanian, A. Mallick, F. Tjiptoharson, S. Rezaei, S. Teo, Q. Zhu, Y. Chen, M. Lin, Z. Dong, K. P. Loh, *Adv. Opt. Mater.* **2023**, *11*, 2202826.
[17] C. Dory, D. Vercruysse, K. Yang, N. Sapra, A. Rugar, S. Sun, D. Lukin, A. Piggott, J. Zhang, M. Radulaski, K. Lagoudakis, L. Su, J. I. Vuckovic, *Nat. Commun.* **2019**, *10*, 3309.
[18] H. Atikian, N. Sinclair, P. Latawiec, X. Xiong, S. Meesala, S. Gauthier, D. Wintz, J. Randi, D. Bernot, S. DeFrances, J. Thomas, M. Roman, S. Durrant, F. Capasso, M. Loncar, *Nat. Commun.* **2022**, *13*, 2610.
[19] S. Fang, W. Guo, Y. Huang, M. Shi, X. Tian, B. Quan, X. Xu, J. Yi, N. Jiang, C. Gu, *iScience* **2024**, *27*, 108939.
[20] M. Kozak, F. Trojanek, B. Rezek, A. Kromka, P. Maly, *Physica E* **2012**, *44*, 1300.
[21] J. Preclikova, A. Kromka, B. Rezek, P. Maly, *Opt. Lett.* **2010**, *35*, 577.
[22] S. Sotoma, C. Zhong, J. Kah, H. Yamashita, T. Plakhotnik, Y. Harada, M. Suzuki, *Sci. Adv.* **2021**, *7*, 7888.
[23] A. Romshin, V. Zeeb, E. Glushkov, A. Radenovic, A. Sinogeikin, *Sci. Rep.* **2023**, *13*, 8546.
[24] R. Simon, J. Pomeroy, M. Kuball, *Appl. Phys. Lett.* **2014**, *104*, 213503.
[25] S. Zhang, S. Li, B. Du, Y. Dong, Y. Zheng, H. Lin, B. Zhao, W. Zhu, G. Wang, X. Chen, G. Guo, F. Sun, *Opt. Mater. Express* **2019**, *9*, 4634.
[26] P. Zhao, H. Wang, F. Kong, Z. Wang, Y. Guo, H. Yu, F. Shi, J. Du, *Adv. Quantum Technol.* **2023**, *10*, 2300191.
[27] X. Gao, C. Yu, S. Zhang, H. Lin, J. Guo, M. Ma, Z. Feng, F. Sun, *Diam. Relat. Mater.* **2023**, *139*, 110348.
[28] H. Yu, Y. Xie, Y. Zhu, X. Rong, J. Du, *Appl. Phys. Lett.* **2020**, *117*, 204002.
[29] J. Jing, F. Sun, Z. Wang, L. Ma, Y. Luo, Z. Du, T. Zhang, Y. Wang, F. Xu, X. Ma, X. Wang, Y. Zhou, J. TSOI, N. Wong, C. Li, D. Ki, K. Li, Y. Lin, Z. Q. Chu, *Nature* **2024**, *636*, 627.
[30] G. Zabow, *Science* **2022**, *378*, 894.
[31] N. Kim, H. Kang, J. Lee, S. Kee, S. Lee, K. Lee, *Adv. Mater.* **2015**, *27*, 2317.
[32] P. Andrich, J. Li, X. Liu, F. Heremans, P. Nealey, D. Awschalom, *Nano Lett.* **2018**, *18*, 4684.
[33] M. Muhammad, S. Buswell, S. Dew, M. Stepanova, *J. Vac. Sci. Technol. B* **2011**, *29*, 06F304.
[34] K. Lim, J. Wi, W. Nam, S. Park, J. Lee, K. Kim, *Nanotechnology* **2009**, *20*, 495303.
[35] L. Bai, V. Mai, Y. Lim, S. Hou, H. Mohwald, H. Duan, *Adv. Mater.* **2018**, *30*, 1705667.

[36] C. Liu, H. Ding, Z. Wu, B. Gao, F. Fu, L. Shang, Z. Gu, Y. Zhao, *Adv. Funct. Mater.* **2016**, *26*, 7937.
[37] L. Zhang, F. Xu, J. Wang, C. He, W. Guo, M. Wang, B. Sheng, L. Lu, Z. Qin, X. Wang, B. Shen, *Sci. Rep.* **2016**, *6*, 35934.
[38] K. Kurematsu, S. Takei, S. Nakajima, K. Mizui, S. Takamatsu, D. Hirata, M. Hanabata, *Microelectron. Eng.* **2019**, *216*, 111085.
[39] M. Modaresialam, N. Granchi, M. Stehlik, C. Petite, S. Delegranu, A. Gourdin, M. Bouabdellaoui, F. Intonti, B. Kerzabi, D. Grosso, L. Gallais, M. Abbarchi, *Opt. Express* **2024**, *7*, 12967.
[40] M. Miyata, H. Hatada, J. Takahara, *Nano Lett.* **2016**, *16*, 3166.
[41] A. Roberts, A. Pors, O. Albrektsen, S. Bozhevolnyi, *Nano Lett.* **2014**, *14*, 783.
[42] D. Sell, J. Yang, S. Doshay, K. Zhang, J. Fan, *ACS Photonics* **2016**, *3*, 1919.
[43] J. Zhu, J. Han, X. Han, S. Meng, A. Liu, X. He, *Opt. Mater.* **2006**, *28*, 473.
[44] Z. Duan, W. Chen, Z. He, J. Yang, D. Wang, Z. Hu, N. Wang, N. Chen, Y. Bu, *Adv. Opt. Mater.* **2024**, *12*, 2301577.
[45] M. Qin, Y. Huang, Y. Li, M. Su, B. Chen, H. Sun, P. Yong, C. Ye, F. Li, Y. Song, *Angew. Chem., Int. Ed.* **2016**, *55*, 6911.
[46] H. Han, J. Oh, H. Lee, S. Lee, S. Mun, S. Jeon, D. Kim, J. Jang, W. Jiang, T. Kim, B. Jeong, J. Kim, D. Ryu, C. Park, *Adv. Mater.* **2024**, *36*, 2310130.
[47] Y. Wu, W. Yang, Y. Fan, Q. Song, S. Xiao, *Sci. Adv.* **2019**, *5*, aax0939.
[48] K. Zhao, J. Cheng, N. Sun, Y. Wang, H. Huang, S. Zhang, W. Niu, *Adv. Mater. Technol.* **2022**, *7*, 2101057.
[49] M. Kong, F. Meng, S. Zhang, B. Tang, *Dyes. Pigm.* **2021**, *195*, 109742.